Available online at www.sciencedirect.com
SCIENCE DIRECT®
Enzyme and Microbial Technology 32 (2003) 407–413
ENZYME and MICROBIAL TECHNOLOGY
www.elsevier.com/locate/enzmictec

# A segregated model for heterologous amylase production by *Bacillus subtilis*

Hanjing Huang [a], Darin Ridgway [a], Tingyue Gu [a,*], Murray Moo-Young [a,b]

[a] *Department of Chemical Engineering, Ohio University, Athens, OH 45701, USA*
[b] *Department of Chemical Engineering, University of Waterloo, Waterloo, Ont., Canada N2L 3G1*

Received 21 June 2002; received in revised form 11 November 2002; accepted 11 November 2002

**Abstract**

A segregated model was proposed to investigate the inherent relationships between growth, substrate consumption, cell differentiation and product formation in a *Bacillus subtilis* fermentation producing heterologous amylase in a 22-l bioreactor. The segregated model includes three distinguishable cell states and the transition from vegetative phase to sporangium and finally to mature spore. An age-based population balance model was applied to describe the maturity of sporangium toward the formation of spores. Parameters in the model were determined by fitting the model with experimental data. The model was able to predict the transient behavior of *B. subtilis* in both batch and fed-batch cultures.


*Keywords:* Population balance; *Bacillus subtilis*; Segregated model

## 1. Introduction

With the development of genetic engineering, *Bacillus subtilis* is becoming a more attractive host to molecular biologists. The advantages of *B. subtilis* such as fast and easy growth high secretion capacity, and non-pathogenic GRAS (Generally Regarded As Safe) status for non-antibiotic producing strains, have made it an attractive host for the production of heterologous enzymes [1,2]. The production of extracellular enzymes by *Bacillus* is associated with differentiation (sporulation) [1].

Efforts have been made to model the production of enzymes by *Bacillus*. In the work by Ollis [3], the exotoxin production by *Bacillus thuringiensis* is described by the Luedeking–Piret equation, and spore formation is a first-order function of the delayed biomass concentration. Shene et al. [4] proposed a simple unstructured model for microbial growth and metabolite production with glucose repression.

A typical structured single-cell model describing the transition from vegetative growth to sporulation incorporates 39 non-linear, differential equations and almost 200 parameters [5]. A segregated model which divides cells into three groups and contains an implicit population balance model for sporangia was first proposed by Dawes and Thornley [6]. They studied the growth and sporulation in continuous culture. This segregated model was further developed by Fordyce and Rawlings [7], who included a two-compartment substrate consumption model and extended the application of their model from steady-state culture to transient growth. However, no enzyme production was included in their model. In this work, a new model was proposed to describe the production of a heterologous thermo-stable amylase by a recombinant *B. subtilis*. The model incorporated both the growth and differentiation of the organism.

## 2. Model development

As shown in Fig. 1, three types of cells exist in a *Bacillus* culture: vegetative cells, sporangia, and spores. When the nutrients are abundant, the vegetative cell can grow quickly by division. When the nutrients are depleted, some of the cells will die, while other cells will survive by differentiating to form sporangia. Sporangia represent the stage of differentiation between the vegetative growth state and the spore state. The entire sporulation process can be divided into seven stages according to morphology and biochemical differences as shown in Table 1 [9]. Many hydrolytic enzymes such as amylase and protease can only be produced during Stage 0 and Stage 2 of sporangium. It takes about 2 h

* Corresponding author. Tel.: +1-740-593-1499; fax: +1-740-593-0873.
*E-mail address:* gu@ohio.edu (T. Gu).

0141-0229/02/$ – see front matter © 2002 Elsevier Science Inc. All rights reserved.
doi:10.1016/S0141-0229(02)00312-5

**Nomenclature**

| | |
|---|---|
| $E$ | amylase concentration (u/l) |
| $F$ | feed rate (l/h) |
| $h$ | step size |
| $k_s$ | saturation constant (g/l) |
| $k_i$ | inhibition constant (g/l) |
| $k_1$ | constant ($h^{-1}$) |
| $k_2$ | constant |
| $k_3$ | constant ($h^{-1}$) |
| $k_d$ | death rate ($h^{-1}$) |
| $k_e$ | amylase production constant (u/cells/h) |
| $m$ | maintenance coefficient (g/cells/h) |
| $S_f$ | glucose concentration in the feed (g/l) |
| $s$ | glucose concentration (g/l) |
| $t_e$ | time between Stage 0 and Stage 2 of sporulation (h) |
| $t$ | time (h) |
| $u(1/2)$ | the $y$ value at the midpoint |
| $V$ | broth volume (l) |
| $x_v$ | vegetative cell number density (cells/l) |
| $x_s$ | sporangium age density function (cells/h/l) |
| $x_s(t)$ | the total sporangium density (cells/l) |
| $x_e$ | spore number density (cells/l) |
| $x_{nonspore}$ | Nonspore number density (cells/l) |
| $Y_{x/s}$ | vegetative cell biomass yield (cells/g) |

*Greek letters*

| | |
|---|---|
| $\mu_{max}$ | maximum specific growth rate ($h^{-1}$) |
| $\mu_v$ | the specific growth rate of vegetative cell ($h^{-1}$) |
| $\mu_s$ | sporulation rate ($h^{-1}$) |
| $\tau_m$ | spore mature time (h) |
| $\tau$ | age of sporangium (h) |

to reach Stage 2 [8,9]. In the work by Dawes and Thornley [6], the mature spore is defined as the appearance of refractivity (the fourth stage of sporulation), which reaches maturity in 4 h. In this work, the definition of a mature spore is Stage 6 of sporulation, in which the cell obtains the resistance properties against heat, chemicals, desiccation and radiation due to its extra outer layers [9]. Some researchers have reported the time to reach maturity is about 7 h [8,9], while other researchers reported that the period for *B. subtilis* to achieve maturity is in the range of 8–10 h [10,11]. When the spore is exposed to a favorable environment, it will germinate to form a vegetative cell.

Table 1
Stages of sporulation in *B. subtilis*

| | |
|---|---|
| Stage 0 | Normal vegetative growth |
| Stage 2 | Asymmetric septation |
| Stage 3 | Prespore protoplast |
| Stage 4 | Cortex formation |
| Stage 5 | Coat formation |
| Stage 6 | Maturation |
| Stage 7 | Release |

Dawes and Thornley [6] concluded that the germination of spores contributes little to the vegetative cell. In the work by Fordyce and Rawlings [7], germination is subject to a time delay of 15 h or more. The spore germination experiment was carried out in this work, and a delay of 7 h for the outgrowth was found. Due to the low spore concentration compared to the vegetative cell concentration, and the time delay for germination and outgrowth, the germination kinetics contribute little to the overall fermentation. Thus, germination kinetics are neglected in this work's model.

Due to the application of selective pressure in the fermentation and the elimination of structural instability from the inoculum, plasmid instability is neglected in the model. The vegetative cell growth model uses Monod growth kinetics. Assuming that only the vegetative cell will consume glucose, the substrate consumption kinetics can be written. The specific rate of sporulation is defined as the rate of the loss of vegetative cell mass due to sporulation. Schaeffer et al. [12] found that the sporulation rate is related to the composition of carbon and nitrogen sources, and a higher glucose concentration will lead to a lower sporulation rate with the same maximum specific growth rate. Dawes and Thornley [6] postulated that the sporulation rate is inversely linear to

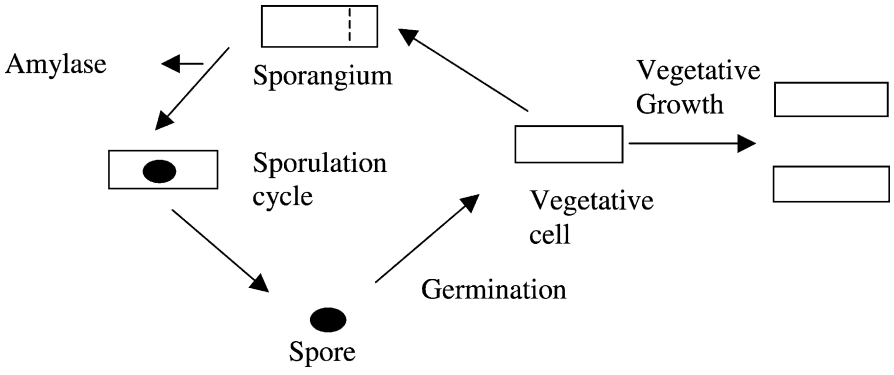


Fig. 1. Life cycle of *B. subtilis* (after Fordyce and Rawlings, 1996).

the specific vegetative growth rate within the dilution rate range from 0.05 to 0.38 $h^{-1}$, corresponding to specific vegetative growth rates from 0.1 to 0.42 $h^{-1}$, and implying the dependence of sporulation on the substrate concentration. Fordyce and Rawlings [7] found that this linear relationship between sporulation rate and specific growth rate did not hold for wider operating conditions. They proposed that the sporulation rate is the linear combination of the piecewise linear basis functions [13]. Fordyce and Rawlings [7] described the dependence of sporulation on the substrate concentration in more detail and fitted the experimental data more accurately for the transient growth. In the work by Fordyce and Rawlings [7] the sporulation rate is inversely linear to the intracellular substrate concentration when the specific vegetative growth rate is above 0.15 $h^{-1}$. When the specific vegetative growth rate is below 0.15 $h^{-1}$, the sporulation rate is linearly related to the intracellular substrate concentration. In this work, the sporulation rate is considered inversely linear to the specific vegetative growth rate when the specific vegetative growth rate is above 0.10 $h^{-1}$, if the specific growth rate is too large, resulting in a negative value for the sporulation rate, the sporulation rate is set to 0. The sporulation rate is linearly related to the specific vegetative growth rate when the specific vegetative growth rate is below 0.10 $h^{-1}$ in this work.

During the sporangium stage, the individual cells from the seven stages of development differ from each other in morphology and biochemistry. A population balance model can describe this heterogeneity. The sporangium age, namely the time since the start of sporulation, is used to characterize the sporangium population based on the stages of spore development. Defining $\tau$ as the sporangium age, and $x_s(\tau, t)$ as the sporangium age density function, according to the definition of a population balance model by Fredrickson et al. [14], and assuming there is no death of the sporangia, a partial differential equation describing the age distribution of the cell population can be written with a birth term included in the boundary condition.

$$\frac{\partial(x_s V)}{\partial t} + \frac{\partial x_s}{\partial \tau} V = 0 \tag{1}$$

$$x_s(0, t) = \mu_s(t) x_v(t) \tag{2}$$

By employing the method of characteristics [15–17], this partial differential equation can be solved analytically and reduced to the ordinary delay differential equation along characteristic trajectories given by $dt/d\tau = 1$.

$$\begin{aligned} x_s(t, \tau) V(t) &= x_s(t - \tau, 0) V(t - \tau) \\ &= \mu_s(t - \tau) x_v(t - \tau) V(t - \tau) \end{aligned} \tag{3}$$

The total number of sporangium cells is the sum of all the cells from age 0 to mature time. The total viable cell number (including vegetative, sporangium, and spore) and spore number can be measured. Only the total nonspore number can be obtained experimentally, and there is no convenient experimental method to distinguish between the vegetative and sporangium cells, except using electron microscopy [7,18,19]. The mature spore formation rate is equal to the sporangium density function at mature time.

For the amylase production kinetics, the glucose repression of amylase production is shown implicitly in the equation, as a high glucose concentration will inhibit the formation of sporangium. In the simplest case, the rate of amylase synthesis is neither substrate nor age dependent, and is considered as constant. The time between Stage 0 and Stage 2 of sporulation is set to 2 h [8,9].

The following equations are written for a fed-batch operation.

Glucose balance:

$$\frac{ds}{dt} = -\left(\frac{\mu_v}{Y_{x/s}} + m\right) x_v + \frac{F(S_f - s)}{V} \tag{4}$$

Vegetative cell number balance:

$$\frac{dx_v}{dt} = (\mu_v - \mu_s) x_v - \frac{F}{V} x_v \tag{5}$$

where,

$$\mu_v = \frac{\mu_{max} s}{k_s + s} \tag{6}$$

For batch culture after glucose is consumed, Eq. (7) is written,

$$\frac{dx_v}{dt} = (-k_d - \mu_s) x_v \tag{7}$$

For $\mu_v \geq 0.1\ h^{-1}$, Eq. (8) is written [6],

$$\mu_s = k_1 - k_2 \mu_v \quad (\mu_v \geq 0.1) \tag{8}$$

$$\mu_s = k_3 + \left(\frac{k_1 - k_3}{0.1} - k_2\right) \mu_v \quad (\mu_v < 0.1) \tag{9}$$

A sporangium number balance is written as [12]:

$$\frac{\partial(x_s V)}{\partial t} + \frac{\partial x_s}{\partial \tau} V = 0 \tag{10}$$

Applying the boundary conditions,

$$x_s(0, t) = \mu_s(t) x_v(t) \tag{11}$$

$$\begin{aligned} x_s(t, \tau) V(t) &= x_s(t - \tau, 0) V(t - \tau) \\ &= \mu_s(t - \tau) x_v(t - \tau) V(t - \tau) \end{aligned} \tag{12}$$

Eq. (10) can be solved analytically to give [7],

So:

$$x_s(t) = \int_0^{\tau_m} \frac{\mu_s(t - \tau) x_v(t - \tau) V(t - \tau)}{V(t)} d\tau \tag{13}$$

When $\tau = \tau_m$, $x_s(t, \tau_m)$ can be obtained from Eq. (9), so the spore number balance can be written as follows.

$$\frac{dx_e}{dt} = \frac{\mu_s(t - \tau_m) x_v(t - \tau_m) V(t - \tau_m)}{V(t)} - \frac{F}{V} x_e \tag{14}$$

$$x_{nonspore} = x_v + x_s(t) \tag{15}$$

The amylase production is written as:

$$\frac{dE}{dt} = \int_0^{t_e} k_e x_s(t, \tau) d\tau - \frac{F}{V}E \quad (16)$$

and the feed rate as:

$$\frac{dV}{dt} = F \quad (17)$$

The model above consists of one ordinary differential equation with a delay term. The Runge–Kutta method can be used to solve a delay differential equation. The Runge–Kutta method provides solutions only at mesh points, while the $x$ value for the delay term may fall between two mesh points. An approximate solution between mesh points should be given. Shampire suggested that the $y$ value be evaluated only at the midpoint, followed by the quartic polynomial interpolation with these values.

Quartic polynomial interpolation is given by:

$$u(0) = y_0 \quad (18)$$

$$u'(0) = hf(x_0, y_0) \quad (19)$$

$$u(1) = y_1 \quad (20)$$

$$u'(1) = hf(x_0 + h, y_1) \quad (21)$$

$$u(1/2) = y_{1/2} \quad (22)$$

In this work, parameter estimation was performed using a Fortran program. First, the initial estimations of the parameters were entered. Then, the simplex subroutine called the objective function, which is the weighted square of the residuals between predicted and experimental values. The predicted values are obtained by calling the subroutine for the delay differential equations. The subroutine for the delay differential equation was obtained by modifying the subroutine provided by Hairer et al. [20].

## 3. Materials and methods

### 3.1. Strain and medium

*B. subtilis* (ATCC 31784) carrying plasmid pC194 was used throughout the study. Plasmid pC194 contains a thermo-stable α-amylase gene from *Bacillus stearothermophilus*. The plasmid also encodes resistance to the antibiotic chloramphenicol (Cm). The host strain does not produce homologous amylase. It produces and secretes heterologous thermo-stable α-amylase into the medium. The genotype for the host strain is phe-tyr-trp-sacA [21], meaning that the strain used in this work cannot synthesize phe, tyr, or trp and sucrose cannot be used as the sole carbon source. The recombinant strain is maintained as spores at 4 °C, on plates of LB selective agar having the following composition: NaCl 10 g/l, yeast extract 5 g/l, tryptone 10 g/l, agar 15 g/l, chloramphenicol 10 mg/l. A defined selective medium containing 10 mg/l chloramphenicol (10 g/l of chloramphenicol dissolved in 100% ethanol and stored in a −20 °C freezer) was used for the batch and fed-batch cultures. Minimum defined medium consisted of (I): $(NH_4)_2SO_4$ 2.5 g/l, $K_2HPO_4$ 3 g/l, $KH_2PO_4$ 1.5 g/l, sodium citrate 1 g/l, $MgSO_4$ 0.25 g/l; (II): $CaCl_2$ 0.1 g/l; (III): $MnSO_4$ 0.01 g/l; (IV): $FeSO_4$ 0.01 g/l; (V): $ZnSO_4$ 0.002 g/l; (VI): Glucose 2 g/l; (VII): phe, tyr, trp 50 mg/l each; and (VIII): chloramphenicol 10 mg/l. I through VII were autoclaved separately, and VIII was filter sterilized.

### 3.2. Culture conditions

*B. subtilis* has two kinds of plasmid instability. One is structural instability, the other is segregational instability. The structural instability of the strain can be eliminated by the plasmid evolution method [22]. Inoculum was prepared in the minimal selective medium containing 10 mg/l chloramphenicol overnight. The inoculation volume was equal to 1% of the initial culture volume in the reactor. The batch and fed-batch cultures were carried out in the minimal selective medium containing 10 mg/l chloramphenicol at 37 °C in a bioreactor (22-l Biostat C, B. Braun Biotech International, GmbH) at a stirring rate of 400 rpm and aeration rate of 1.5 vvm.

### 3.3. Biomass assay

The sample was kept in an 80 °C water bath for 10 min to kill the nonspore cells, and then both the heated and unheated samples were serially diluted using sterile saline water. The diluted samples were put on plates, and then the LB agar was poured onto the plates. Plates were incubated overnight at 37 °C.

### 3.4. Glucose assay

Glucose concentrations were determined using a glucose assay kit from Sigma (Kit No. 510) (St. Louis, MO).

### 3.5. Amylase assay

A total of 0.5 ml enzyme solution and 0.5 ml starch (1%) in 0.1 M NaAC (pH 6.0) were mixed and allowed to react at 40 °C for 30 min. A total of 2 ml DNS reagent [23] were added to stop the reaction and the samples was incubated at 100 °C for 10 min. (The DNS reacts with the reducing sugars released by the amylase.) The control was a tube with the DNS reagent and inactivated enzyme (boiled) or with enzyme added after incubation. Reducing sugar was determined by comparing adsorption at 540 nm of the assay solution to a standard curve of glucose solutions (1–10 mg/ml). One unit of amylase activity was defined as the release of 1 μmol reducing sugar from the soluble starch per minute.

The preparation of DNS reagent was as follows: Over gentle heat, dissolve 10 g 3,5-dinitrosalicylic acid in 200 ml NaOH (2N) while gradually adding 500 ml water, then add

300 g potassium sodium tartrate. Bring the total volume up to 1 l with water and store at room temperature in a dark colored bottle.

## 4. Results and discussion

### 4.1. Batch culture with cell lysis

The time courses of the concentrations of glucose, amylase, nonspore, and spore cells are shown in Fig. 2. Cell lysis occurred immediately after glucose was depleted, which is consistent with the report for *Bacillus amyloliquefaciens* by Ponzo and Weigand [24]. In their work, they noticed that no apparent degradation of amylase by protease was found during the cell lysis. An extension to the cell lysis phase was needed to study the spore formation kinetics and thermo-stable amylase production kinetics. As shown in Fig. 2, the thermo-stable amylase activity increased shortly after the depletion of glucose, while the spore formation showed a longer delay. Parameters were determined by fitting the data with the model, and are listed in Table 2.

In their work [7], Fordyce and Rawlings first examined the sporulation rate in batch culture, then used a piecewise linear basis function to describe the relationship between the sporulation rate and intracellular substrate concentration. They found that the sporulation rate was relatively sensitive for the batch run when the maximum death rate was reached, namely the zero intracellular substrate concentration. At the other non-zero substrate concentrations, they set the sporulation rate to 0. This rough description of the sporulation rate resulted in a poor fit of data for the step-test. So in their work, the growth and sporulation parameters were re-estimated using both the batch and step-test data by putting a relatively dense linear element near the zero intracellular substrate concentration. They found that there existed a maximum sporulation rate near the zero intracellular substrate concentration equal to $0.042\,h^{-1}$ by drawing the graph of the sporulation rate versus intracellular substrate concentration. This implied that there existed a maximum sporulation rate around a dilution rate of $0.15\,h^{-1}$ (calculated in this work for his case). The newly established sporulation rate as a function of the intracellular substrate concentration could fit the step-test data well. However, they did not show the fit to the batch data.

Table 2
Summary of experimentally determined parameters

| Parameter | Value |
|---|---|
| $\mu_{max}$ ($h^{-1}$) | 0.72 |
| $k_s$ (g/l) | 0.10 |
| $Y_{x/s}$ (cells/g) | $6.0 \times 10^{11}$ |
| $m$ (g/cells/h) | $2.5 \times 10^{-14}$ |
| $k_d$ ($h^{-1}$) | 0.150 |
| $k_1$ ($h^{-1}$) | 0.003 |
| $k_2$ | 0.005 |
| $k_3$ ($h^{-1}$) | $1.95 \times 10^{-4}$ |
| $\tau_m$ (h) | 8 |
| $k_e$ (u/cells/h) | $2.6 \times 10^{-6}$ |

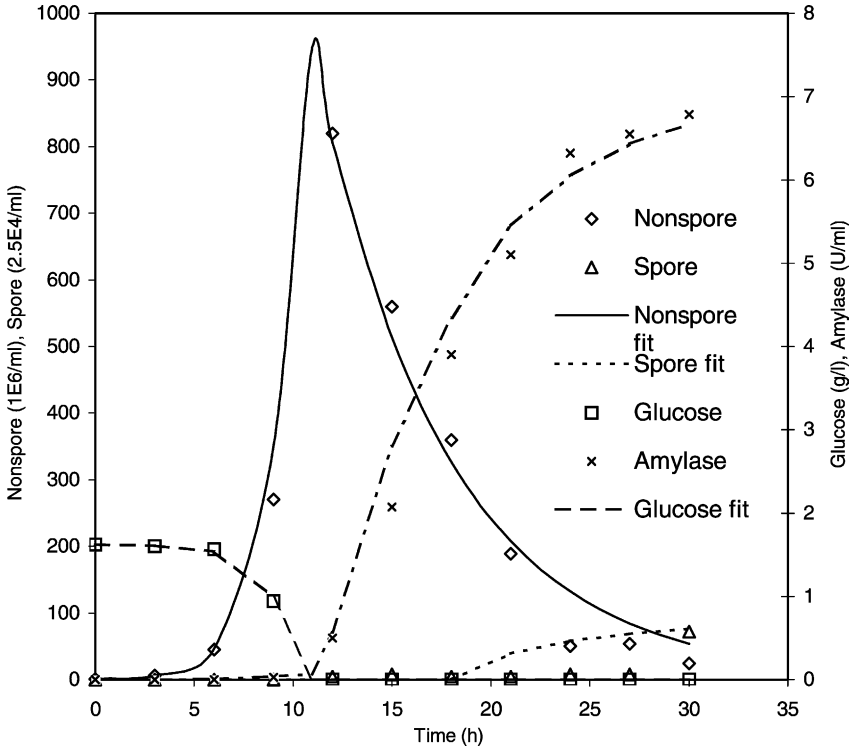


Fig. 2. Batch culture with cell lysis.

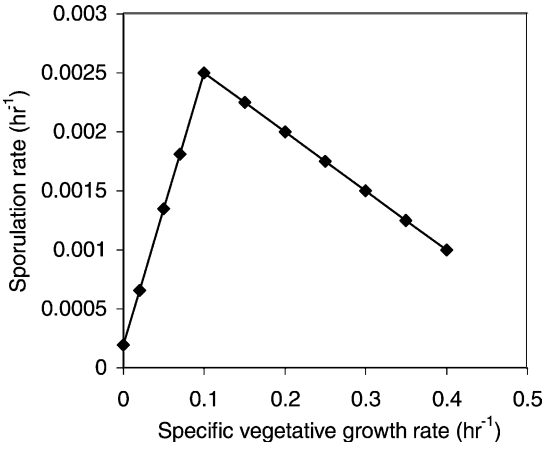


Fig. 3. Sporulation rate vs. specific vegetative growth rate.

In this work, the simulation result for the sporulation rate versus the specific vegetative growth rate is shown in Fig. 3, and the simulation result for the sporulation rate versus glucose concentration is shown in Fig. 4. The lower value for the sporulation rate compared to the work of Dawes et al. may be due to the different strain type and the presence of amino acids in the medium that may inhibit the sporulation [12]. The fitting of the batch data in this work was reasonably good, and a better fit of amylase production could be achieved by further adjusting the rate of amylase production while fixing the other parameters. The unstructured glucose inhibition model proposed by Shene et al. [4] was applied to this system as a comparison between models. From the parameter estimation and simulation results, the unstructured glucose inhibition model will result in the earlier take-off

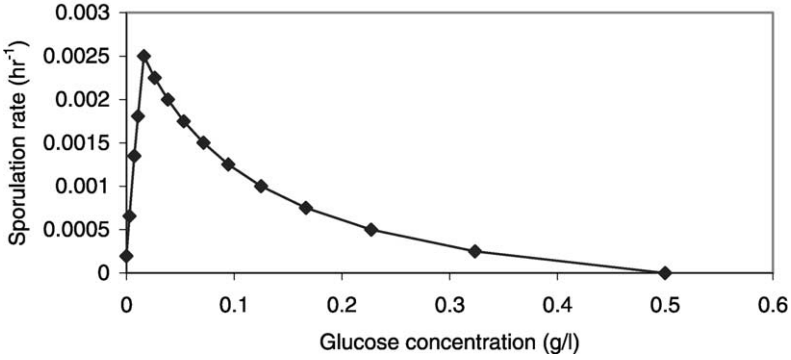


Fig. 4. Sporulation rate vs. glucose concentration.

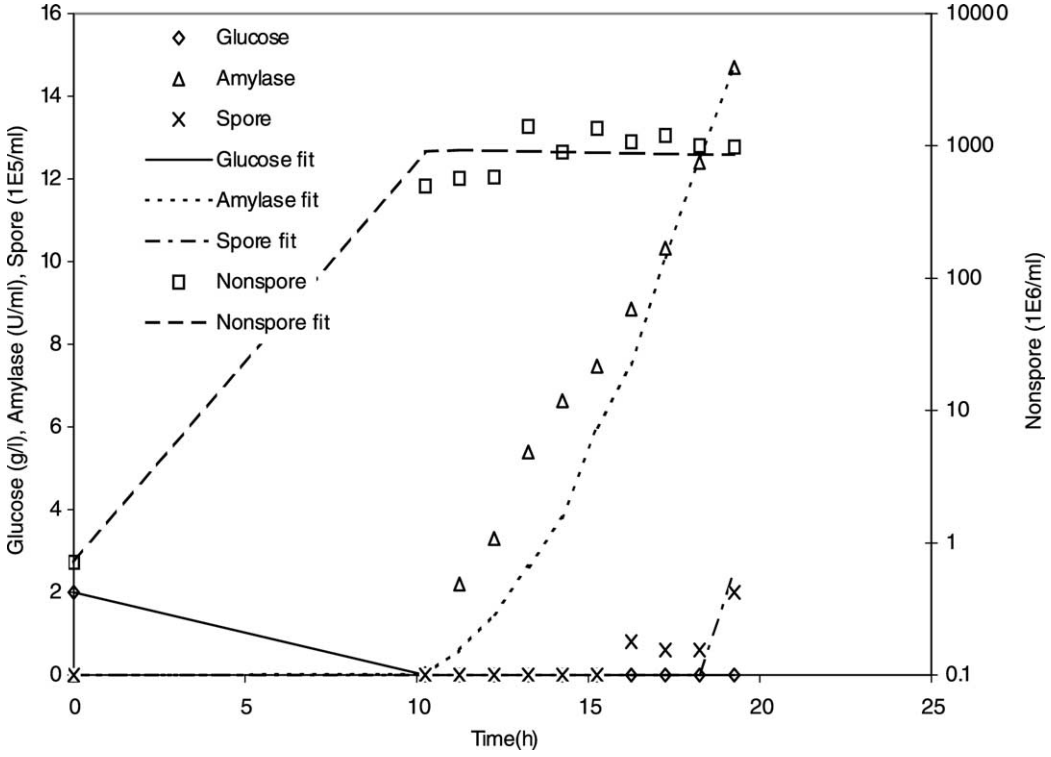


Fig. 5. Fed batch culture with constant feed, feed rate is $0.18\,l\,h^{-1}$, broth volume when feed starts is 6 l, and constant inlet substrate concentration is $2\,g\,l^{-1}$.

of the thermo-stable amylase and much flatter curve at the later stage for the batch run with cell lysis.

### 4.2. Batch and constant feed

As shown in Fig. 5, after the batch phase was over, constant feeding started with a glucose concentration of 2 g/l in the feed. The feed rate was low such that the dilution rate during the fed-batch culture was below 0.12 $h^{-1}$, which was the threshold for accumulation of acetate reported by Snay et al. [25]. The nonspore concentration was maintained around a constant value in the constant feed phase after the rapid increase during the batch phase. The much higher enzyme production rate was obtained in the constant feed phase at the low constant feed rate (0.18 l $h^{-1}$) as compared to the one at cell lysis phase in Fig. 2. Slight adjustment of some parameters determined from batch culture with cell lysis gave a better simulation result for nonspore, glucose, amylase and spore concentration as shown in Fig. 5. In Fig. 5, it can be seen that the model fits the data well, and it further tests the sporulation kinetics around very low substrate concentrations.

There is another kind of recombinant *B. subtilis* in which the sporulation process is blocked at Stage 2, and the recombinant protein is produced during the period from Stage 0 to Stage 2, and no spore is formed. This kind of strain has been reported by Oh et al. [8] for subtilisin production by *B. subtilis DB104*(Δ*npr* Δ*apr*) (*Em*$^r$) *spoIIG*(*BIm*$^r$):: *pMK101*(*Cm*$^r$) in fed-batch and continuous cultures, also in Pierce et al. [18] for subtilisin production by *B. subtilis* RS7907 in fed-batch culture. The model presented in this work can also be applied to this kind of strain and it helps to explain the increased production capabilities for this kind of asporogenous strain by extending the production phase as compared to the wild-type sporogenous strain.

## 5. Conclusions

The model proposed in this work can successfully describe the differentiation phenomenon with associated product formation in both batch culture and fed-batch culture. The model parameters were determined from the experimental data of the batch culture, and only slight adjustments of some parameters were needed to simulate the fed batch culture. The model can be used for the optimization of enzyme production. The model may also help to understand the increased production capabilities for the asporogenous strain by extending the production phase.

## References

[1] Mountain A. Gene expression system for *Bacillus subtilis*. In: Harwood CR, editor. *Bacillus*. New York: Plenum Press; 1989. p. 73–4.
[2] Deboer AS, Diderichsen B. On the safety of *Bacillus subtilis* and *B. amyloliquefaciens*: a review. Appl Microbiol Biotechnol 1991;36:1–4.
[3] Ollis DF. A simple batch fermentation model: theme and variations. Ann N Y Acad Sci 1983;413:144–56.
[4] Shene C, Andrews BA, Asenjo JA. Fedbatch fermentations of *Bacillus subtilis* ToC46(pPFF1) for the synthesis of a recombinant β-1,3-glucanase: experimental study and modeling. Enzyme Microb Technol 1999;24(5/6):247–54.
[5] Jeong JW, Snay J, Ataai MM. A mathematical model for examining growth and sporulation processes of *Bacillus subtilis*. Biotechnol Bioeng 1990;35(2):160–84.
[6] Dawes IW, Thornley JHM. Sporulation in *Bacillus subtilis*. Theoretical and experimental studies in continuous culture systems. J Gen Microbiol 1970;62:49–66.
[7] Fordyce AP, Rawlings JB. Segregated fermentation model for growth and differentiation of *Bacillus licheniformis*. AIChE J 1996;42(1):3241–52.
[8] Oh MK, Kim BG, Park SH. Importance of spore mutants for fedbatch and continuous fermentation of *Bacillus subtilis*. Biotechnol Bioeng 1995;47:696–702.
[9] Doi RH. Sporulation and germination. In: Harwood CR, editor. *Bacillus*. New York: Plenum Press; 1989. p. 169–215.
[10] Nicholson WL, Setlow P. Sporulation, germination and outgrowth. In: Harwood CR, Cutting SM, editors. Molecular biology methods for *Bacillus*. New York: Wiley; 1990. p. 391–450.
[11] Losick R, Youngman P. Endospore formation in *Bacillus*. In: Losick R, Shapiro L, editors. Microbial development. Cold Spring Harbor, NY: Cold Spring Harbor Laboratory; 1984. p. 63.
[12] Schaeffer P, Millet J, Aubert JP. Catabolic repression of bacterial sporulation. Microbiology 1965;54:704–11.
[13] Reddy JNN. An introduction to the finite element method. New York: McGraw-Hill; 1992.
[14] Fredrickson AG, Ramkrishna D, Tsuchiya HM. Statistics and dynamics of prokaryotic cell populations. Math Biosci 1967;1:327–74.
[15] Haberman R. Elementary applied partial differential equations. 3rd ed. Englewood Cliffs, NJ: Prentice-Hall; 1998.
[16] Ramkrishna D. Statistical models of cell populations. Adv Biochem Eng 1979;11:1–47.
[17] Liou JJ, Srienc F, Fredrickson AG. Solution of population balance models based on a successive generations approach. Chem Eng Sci 1997;52(9):1529–40.
[18] Pierce JA, Robertson CR, Leighton TJ. Physiological and genetic strategies for enhanced subtilisin production by *Bacillus subtilis*. Biotechnol Prog 1992;8(3):211–7.
[19] Tanimoto Y, Ichikawa Y, Yasuda Y, Tochikubo K. Permeability of dormant spores of *Bacillus subtilis* to gramicidin S. FEMS Microbiol Lett 1996;136:151–6.
[20] Hairer E, Norsett SP, Wanner G. Solving ordinary differential equations. 2nd ed. New York: Springer; 1993.
[21] Mielenz JR, Mickel S. Process for cloning the gene coding for a thermostable apha-amylase into *Escherichia coli* and *Bacillus subtilis*. US Patent No. 4,493,893 (1985).
[22] Wei D, Parulekar SJ, Stark BC, Weigand WA. Plasmid stability and α-amylase production in batch and continuous cultures of *Bacillus subtilis* TN106[pAT5]. Biotechnol Bioeng 1989;33:1010–20.
[23] Park Y, Uehara H, Teruya R, Okabe M. Effect of culture temperature and dissolved oxygen concentration on expression of α-amylase gene in batch culture of spore-forming host *Bacillus subtilis* 1A289. J Ferment Bioeng 1997;84:53–8.
[24] Ponzo JH, Weigand WA. Simple structured model for α-amylase synthesis by *Bacillus amyloliquefaciens*. Biotechnol Bioeng 1991;38:1065–81.
[25] Snay J, Jeong JW, Ataai MM. Effects of growth conditions on carbon utilization and organic by-product formation in *B. subtilis*. Biotechnol Prog 1989;5:63–9.